The Astrophysical Journal Letters, 836:L7 (6pp), 2017 February 10 doi:10.3847/2041-8213/836/1/L7

The Chemical Composition of an Extrasolar Kuiper-Belt-Object*

S. Xu (许偲艺)[1], B. Zuckerman[2], P. Dufour[3], E. D. Young[4], B. Klein[2], and M. Jura[2]
[1] European Southern Observatory, Karl-Schwarzschild-Straße 2, D-85748 Garching, Germany; sxu@eso.org
[2] Department of Physics and Astronomy, University of California, Los Angeles, CA 90095-1562, USA
[3] Institut de Recherche sur les Exoplanètes (iREx) and Département de physique, Université de Montréal, Montréal, QC H3C 3J7, Canada
[4] Department of Earth, Planetary, and Space Sciences, University of California, Los Angeles, CA 90095, USA
Received 2016 October 6; revised 2016 December 20; accepted 2017 January 5; published 2017 February 9

Abstract

The Kuiper Belt of our solar system is a source of short-period comets that may have delivered water and other volatiles to Earth and the other terrestrial planets. However, the distribution of water and other volatiles in extrasolar planetary systems is largely unknown. We report the discovery of an accretion of a Kuiper-Belt-Object analog onto the atmosphere of the white dwarf WD 1425+540. The heavy elements C, N, O, Mg, Si, S, Ca, Fe, and Ni are detected, with nitrogen observed for the first time in extrasolar planetary debris. The nitrogen mass fraction is ∼2%, comparable to that in comet Halley and higher than in any other known solar system object. The lower limit to the accreted mass is $\sim 10^{22}$ g, which is about one hundred thousand times the typical mass of a short-period comet. In addition, WD 1425+540 has a wide binary companion, which could facilitate perturbing a Kuiper-Belt-Object analog into the white dwarf's tidal radius. This finding shows that analogs to objects in our Kuiper Belt exist around other stars and could be responsible for the delivery of volatiles to terrestrial planets beyond the solar system.

Key words: Kuiper belt: general – planetary systems – stars: abundances – white dwarfs

Supporting material: data behind figure

1. Introduction

Volatile elements, such as nitrogen, carbon, and oxygen are crucial for the chemistry of life. The prevalence of water is of particular importance. The distributions of water and other volatiles in our solar system were controlled primarily by temperatures in the protoplanetary disk (McSween & Huss 2010). Interior of the snow line in the disk, water remained in the gas phase, and rocks were, consequently, relatively dry. Beyond the snow line, water was stable as ice, vestiges of which persist to this day in some asteroids, icy moons, comets, and Kuiper-Belt-Objects (KBOs). Even further out, nitrogen ice condensed into rocks and could be present in comets from the Kuiper Belt and Oort Cloud.

It is commonly argued that terrestrial planets, having formed inside of the snow line, may have accreted from dry refractory materials, and that water and other volatile compounds were delivered later by the impact of planetesimals from the asteroid belt and/or Kuiper Belt (Morbidelli et al. 2000). The presence of KBOs around other stars has been inferred by excess ∼50 K blackbody radiation (e.g., Beichman et al. 2006). However, the concentrations of water and other volatiles within such extrasolar minor bodies are largely unknown.

The sizes and masses of some individual extrasolar planets can be measured when combining radial velocity and transit observations (e.g., Pepe et al. 2013). Therefore, the bulk density of an extrasolar planet can be inferred, but it is difficult to find a unique solution for the planet's internal composition (Dorn et al. 2015). Recently, it has been shown that many white dwarfs are actively accreting rocky debris that "pollutes" their atmospheres (Zuckerman et al. 2003, 2010; Koester et al. 2014). Typically, a white dwarf's atmosphere is dominated by either hydrogen or helium because heavier elements sink due to the high surface gravity. Heavy elements, if detected, must therefore come from an external source, and in many cases that source is an accretion of a tidally disrupted rocky object (Jura 2003). As a result, high-resolution spectroscopic observations of polluted white dwarfs provide a unique way to measure the bulk compositions of extrasolar planetary objects (Jura & Young 2014).

There are at least a dozen polluted white dwarfs with detailed measurements of accreted material (Jura & Young 2014). Their abundance patterns are similar to those of rocky objects in our solar system, including bulk Earth and chondrite meteorites from the asteroid belt—O, Fe, Si, and Mg are the four dominant elements in familiar proportions. Volatile elements are almost always depleted, just as they are in Earth and meteorites from the asteroid belt (Gänsicke et al. 2012; Jura et al. 2012; Xu et al. 2014). Excess oxygen relative to which can be bound to rock-forming elements like Mg, Si, Fe, and Ca has only been detected in three white dwarfs. The excess oxygen is attributable to accretion of H_2O rich objects (Farihi et al. 2013). The rarity of water among the objects sampled by polluted white dwarfs to date is likely to be an indicator of low primordial water content because water and volatiles are generally expected to survive the post main sequence evolution of the host star (Jura & Xu 2010; Malamud & Perets 2016). In general, the overall compositions of extrasolar rocky material identified thus far closely resemble those of dry, relatively volatile-poor asteroids in our solar system.

Here, we report results of high-resolution spectroscopic observations of the polluted white dwarf WD 1425+540 with the *Keck Telescope* and the *Hubble Space Telescope*. WD 1425+540 (G200-39, 14:27:36.0, +53:48:28.4 J2000) was first reported in Greenstein's degenerate star catalog (Greenstein 1974). It has a K dwarf companion G200-40 located 40.0 arcsec away at

* Part of the data presented herein were obtained at the W.M. Keck Observatory, which is operated as a scientific partnership among Caltech, the University of California and NASA. The Observatory was made possible by the generous financial support of the W.M. Keck Foundation.

14:27:37.1, +53:47:49.2 J2000 (Wegner 1981).[5] WD 1425+540 has a helium-dominated atmosphere but also contains a large amount of hydrogen; it is the prototype of the "DBA" class of white dwarfs that display both helium and hydrogen lines (Liebert et al. 1979; Jura & Xu 2012).

2. Observations and Data Reduction

2.1. High-Resolution Echelle Spectrograph (HIRES)

WD 1425+540 was observed with the blue collimator of the HIRES (Vogt et al. 1994) on the *Keck Telescope* on 2008 February 13 and 2014 May 22 (UT). The weather was clear on both nights. The C5 decker was used, and the resolution was ~40,000. The total exposure time was 5960 s. Data were reduced using standard IRAF routines developed for reducing echelle data following Klein et al. (2010). The final combined spectrum has an almost continuous coverage from 3115 to 5960 Å.

2.2. HST/Cosmic Origins Spectrograph (COS)

WD 1425+540 was observed with the COS on board the *Hubble Space Telescope* under program ID 13453 (PI: M. Jura) on 2014 December 8 (UT). We used the G130M grating with a central wavelength of 1291 Å, which gives a wavelength coverage of 1130–1431 Å with a small gap in the middle. The spectral resolution was ~20,000. We had five consecutive orbits on this star and the total exposure time was 8358 s. The data were processed with the pipeline CALCOS 2.18.5. Following Jura et al. (2012), around the O I triplet 1304 Å region, we used the timefilter to extract the night-time portion of the data to minimize the effect of geocoronal emissions.

2.3. Abundance Analysis

WD 1425+540 has a trigonometric parallax and the derived distance is 58 ± 13 pc (van Altena et al. 1995). Bergeron et al. (2011) fitted the optical spectra and found the effective temperature $T_{\rm eff}$ = 14,490 K, surface gravity $\log g = 7.95$, and the hydrogen to helium ratio $\log n({\rm H})/n({\rm He}) = -4.2$. They also derived a spectroscopic distance of 56 pc, in good agreement with the parallax. However, this model cannot reproduce the strong asymmetric Lyα in the *COS* data (Genest-Beaulieu & Bergeron 2016).

Lyα can be contaminated with interstellar absorption, which makes it stronger than expected from the optical hydrogen abundance. An interstellar hydrogen column density of $\sim 10^{22}$ cm^{-2} is required to fit the red wing of Lyα. However, the Schlegel map shows that the extinction $E(B-V)$ is 0.02 along the line of sight of WD 1425+540 (Schlegel et al. 1998). That corresponds to an upper limit of the hydrogen column density of 10^{20} cm^{-2}, which is two orders of magnitude smaller than the amount of H required to fit Lyα. Thus, interstellar absorption along the line of sight cannot explain the order of magnitude discrepancy between the model-derived optical and ultraviolet hydrogen abundances.

In order to search for a solution that fits all of the observed parameters, we computed a grid of models that cover $T_{\rm eff}$ between 13,000 K and 16,500 K, $\log g$ between 7.5 and 9.0, and $\log n({\rm H})/({\rm He})$ between −3.0 and −5.0. We compared the models with the observed SED, He lines, Balmer lines, and Lyα. However, we were unable to find a solution that fits all of the observables; the discrepancy between Balmer lines and Lyα is always present. WD 1425+540 represents an extreme case, but discrepancies between optical and ultraviolet hydrogen abundances have been observed in other helium-dominated white dwarfs (e.g., Jura et al. 2012). Genest-Beaulieu & Bergeron (2016) investigated this issue and found it is possibly due to atmospheric stratification. Finding the best white dwarf parameters that fit all available data is beyond the scope of this paper, and we defer it to a future study. Fortunately, the relative element abundances are not sensitive to white dwarf parameters for white dwarfs like WD 1425+540; they are comparable within the measurement uncertainties (Klein et al. 2010, 2011).

We adopted the temperature and surface gravity as listed in Bergeron et al. (2011). To assess the effect of hydrogen abundance on the heavy elements, we calculated synthetic white dwarf model spectra for two sets of hydrogen abundances: model I adopts $\log n({\rm H})/n({\rm He}) = -4.2$, as derived from Balmer lines, while model II uses $\log n({\rm H})/n({\rm He}) = -3.0$ from Lyα.[6] To derive the abundances of heavy elements, we followed the method outlined in Dufour et al. (2010, 2012) and divided the spectra into 10–20 Å segments. Each element typically has 2–4 segments and each segment was fitted separately, as shown in Figure 1. The flux level of the model in each segment was another free parameter; this was particularly important for the lines in the wings of Lyα (e.g., Figure 1, panels (d), (e), (f), and (g)), because we were not able to reproduce the asymmetric profile of Lyα. We used a chi-squared minimization routine to iterate our calculation of the model atmosphere until the difference between the observed spectra and the model reached the minimum. The uncertainty was calculated by taking the standard deviation of the abundances derived from each segment. Some representative spectra are shown in Figure 1. Both the *COS* data and the model spectra are available in the supplementary material.

At 58 pc, there can still be a small amount of interstellar absorption present in the ultraviolet spectra of WD 1425+540. The average radial velocity of the stellar spectral lines is 3.0 ± 4.8 km s^{-1}, very close to the velocity of typical interstellar lines. In order to assess the potential influence of interstellar lines, we only fit lines that are most likely to have an interstellar contribution based on previous studies (Jura et al. 2012); these include Si II 1260.4 Å, C II 1334.5 Å, O I 1302.2 Å, and the N I triplet around 1200 Å. We found the derived abundances based on these lines to be comparable to those from the other photospheric lines. We conclude that interstellar lines do not contribute significantly to the spectra, and we used all available lines, as also seen in previous studies (Gänsicke et al. 2012; Jura et al. 2012), to derive the final abundances reported in Table 1. Specifically, the abundance of N is derived from N I 1243.2 Å (panel (f) in Figure 1), the N I triplet around 1200 Å (panel (e) in Figure 1), and the N I triplet around 1145 Å.

To derive the intrinsic abundances in the accreting material, we need to know the stage of the accretion process. The accretion of material onto a white dwarf has been classified into three stages, the build-up phase, the steady-state stage, and the

[5] The naming of these two objects is confusing in the literature and sometimes WD 1425+540 has been mistakenly referred to as G200-40.

[6] Genest-Beaulieu & Bergeron (2016) considered a pure helium atmosphere and derived $\log n({\rm H})/n({\rm He}) = -2.63$ for Lyα, which is different from our value of −3.0. It is likely due to the presence of heavy elements, which changes the temperature and pressure profile of the atmosphere (e.g., Dufour et al. 2010).

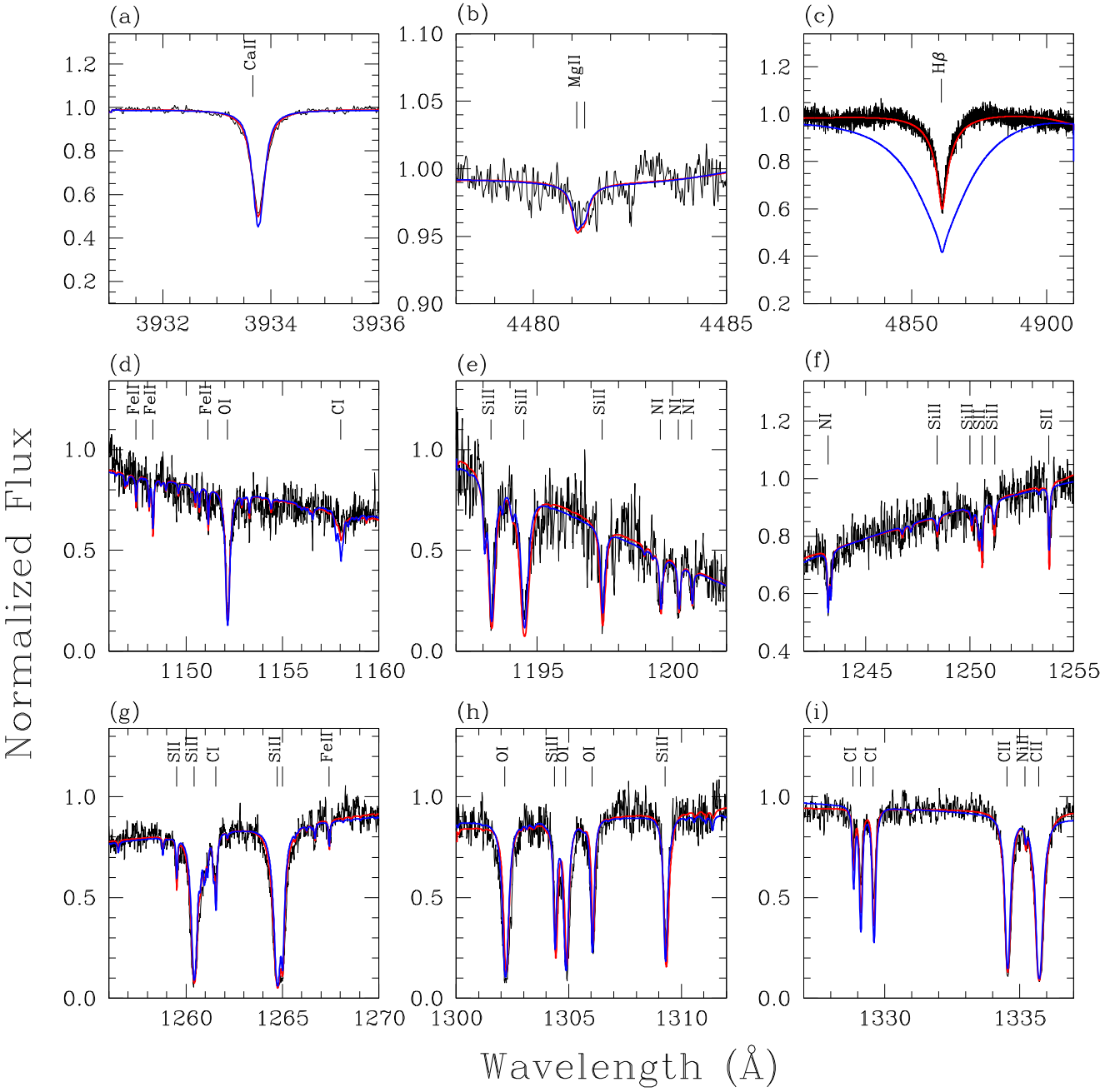

Figure 1. Representative spectra for WD 1425+540. The black line represents the data, while the red (model I) and blue (model II) lines are our model fit with abundances from Table 1. The top panels are from Keck/HIRES, while the rest are from *HST*/COS. Some weak Fe II lines are not labeled. The data used to create this figure are available.

dissipating stage (Koester 2009). The steady-state accretion is sometimes accompanied by the presence of infrared excess from a circumstellar dust disk. The dissipating stage often shows an under-abundance of heavier elements, such as Ca, Fe, and Ni, due to their relatively short settling times.[7] WD 1425 +540 does not have an infrared excess, and the abundance ratios between Ca, Fe, and Ni relative to Mg are "normal," compared to other rocky objects. We derive the compositions of the accreting material in both the build-up and steady-state stages, as shown in Table 2. Our main conclusion of accretion from a volatile-rich object is not dependent on the assumption of a particular accretion stage, because the difference in settling times is, at most, a factor of 1.7 (between C and Fe, see Table 1).

[7] For example, see Table 1 for settling times of different elements and Jura & Xu (2012) for discussion about dissipating stage accretion for GD 61.

3. Discussion

Tables 1 and 2 provide abundances and mass fractions for C, N, O, Mg, Si, S, Ca, Fe, and Ni. The overall abundance pattern derived from these data resembles the composition of comet Halley, as shown in Figure 2. The volatile elements nitrogen, carbon, and oxygen are enhanced relative to those in bulk Earth and CI chondrites. The relative abundances of rock-forming

Table 1
WD 1425+540 Abundances

Element	log n(Z)/n(He)[a]		log t[b](year)	M[c] (10^{20} g)		$\dot{M}$[d] (10^{7} g s^{-1})	
	I	II	I and II	I	II	I	II
H	−4.20 ± 0.10	−3.00 ± 0.10	...	1130	1790	...	...
C	−7.29 ± 0.17	−7.28 ± 0.31	6.164	11.0	11.4	2.41	2.48
N	−8.09 ± 0.10	−7.97 ± 0.15	6.123	2.06	2.67	0.50	0.64
O	−6.62 ± 0.23	−6.51 ± 0.22	6.113	68.5	89.2	16.7	21.8
Mg	−8.16 ± 0.20	−8.11 ± 0.20	6.115	2.99	3.32	0.73	0.81
Si	−8.03 ± 0.31	−7.87 ± 0.26	6.106	4.66	6.72	1.16	1.67
S	−8.36 ± 0.11	−8.13 ± 0.16	6.032	2.48	4.26	0.73	1.25
Ca	−9.26 ± 0.10	−9.31 ± 0.10	5.935	0.40	0.35	0.15	0.13
Fe	−8.15 ± 0.14	−7.99 ± 0.10	5.925	7.02	10.3	2.65	3.90
Ni	−9.67 ± 0.20	−9.52 ± 0.20	5.940	0.28	0.32	0.08	0.12
Total[e]	...	...	...	99.4	128.6	25.1	32.8

Notes. We present results for two models I and II (see Section 2.3).
[a] Measured abundances in the convective zone. The mass of the convection zone relative to the total mass of the white dwarf, $q = \log M_{cvz}/M_{WD} = -5.495$.
[b] Settling times out of the convective zone (Dufour et al. 2016).
[c] The total mass of each element that is currently in the convective zone.
[d] The average accretion rate of each element, calculated by dividing the mass of an element M by its settling time t.
[e] Only the heavy elements are included in this row. H is excluded.

Table 2
Mass Fractions of Heavy Elements in Different Rocky Objects

Element	WD 1425+540				Comet Halley	Bulk Earth	CI Chondrites
	I. bd	I. std	II. bd	II. std			
C	11.2%	9.6%	8.9%	7.6%	25.8%	0.17%–0.39%	3.2%
N	2.1%	2.0%	2.1%	1.9%	1.6%	1.2e-6	0.15%
O	68.9%	66.7%	69.4%	66.5%	37.6%	32.4%	46.0%
Mg	3.0%	2.9%	2.6%	2.5%	6.3%	15.8%	9.7%
Si	4.7%	4.6%	5.2%	5.1%	13.7%	17.1%	10.5%
S	2.5%	2.9%	3.3%	3.8%	6.1%	0.46%	5.9%
Ca	0.4%	0.6%	0.3%	0.4%	0.7%	1.62%	0.92%
Fe	7.1%	10.5%	8.0%	11.9%	7.7%	28.8%	18.2%
Ni	0.2%	0.3%	0.3%	0.4%	0.6%	1.69%	1.07%

Note. The mass fraction of WD 1425+540 is shown assuming build-up (bd), steady-state (std) accretion, $\log n(\mathrm{H})/n(\mathrm{He}) = -4.2$ (model I), and −3.0 (model II), respectively. H is excluded in the calculations because much or most of the hydrogen may not be associated with the current accretion event (Jura & Xu 2012). If we take the amount of hydrogen that could have been bound with the excess oxygen (55% by number, see Section 3), in the form of H_2O, then the mass fraction of hydrogen would be ∼5%, which is comparable to that in comet Halley 5% (Jessberger et al. 1988). In that case, the mass fraction of other heavy elements would be slightly lower. The mass fractions of different elements, excluding H, for a few solar system objects are also listed (Jessberger et al. 1988; Wasson & Kallemeyn 1988; Allègre et al. 2001).

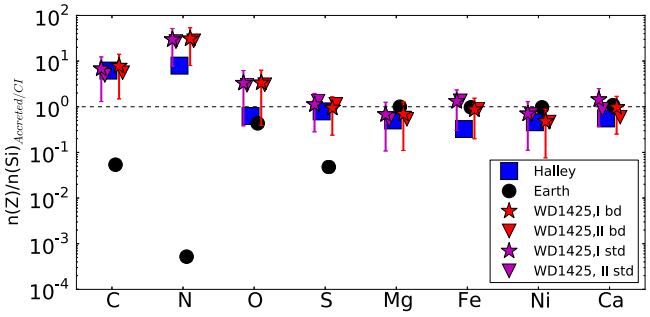

Figure 2. Number fraction of various elements relative to silicon, a major constituent of rocky planetary material in our solar system. The ratios have been normalized to that of CI chondrites representing standard solar-system abundances of rock-forming elements. Four models are shown for the composition of the material accreting onto WD 1425+540; model I for $\log n(\mathrm{H})/n(\mathrm{He}) = -4.2$, model II for $\log n(\mathrm{H})/n(\mathrm{He}) = -3.0$, the build-up accretion model (bd), and the steady-state accretion model (std, see Table 2). For clarity, error bars are not shown for model II but they are comparable to those in model I. In all cases, the composition of the material accreting onto WD 1425+540 resembles that of comet Halley.

elements in WD 1425+540, including Si, Mg, Ca, Ni, and Fe, are similar to chondritic rocks of our solar system. The total mass of heavy elements in the convective zone of WD 1425+540 is $\sim 10^{22}$ g; this is about 0.10% of the mass of the most massive KBO Pluto (Buie et al. 2006). The mass in the convective zone represents a lower limit to the total accreted mass, and the accreting object could have been more massive.

The solar-like abundance of nitrogen for the object accreted onto WD 1425+540 is higher than existing quantitative estimates of N in chondrites and Earth (see Figure 3). Bulk nitrogen concentrations are largely unknown for outer solar system bodies, but nitrogen ice is prevalent on the surface of cold KBOs, including Pluto, Charon, and Eris due to the stability of N_2 and ammonia ices at cold temperatures (Cruikshank et al. 2015). We conclude that the abundant nitrogen present in WD 1425+540 is a signature of formation beyond the nitrogen ice line in a location analogous to our Kuiper Belt. This first detection of nitrogen in a white dwarf

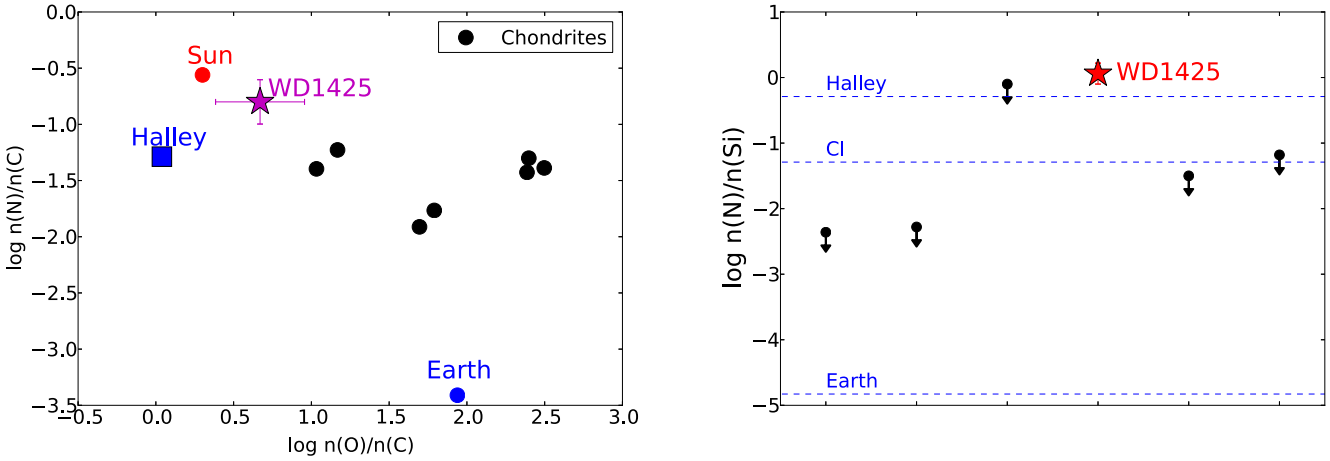

Figure 3. Left panel: N/C vs. O/C ratios by number for chondrites (Wasson & Kallemeyn 1988), the Sun (Lodders 2003), comet Halley (Jessberger et al. 1988), bulk Earth (Allègre et al. 2001), and WD 1425+540. The abundance ratios from different models of WD 1425+540 all lie within the error bars. WD 1425+540 has accreted materials with abundance ratios of volatile elements similar to those of the Sun and comet Halley, which are different from rocky objects in the solar system (Jura & Young 2014). Right panel: black dots are upper limits to N/Si ratios by number for some polluted white dwarfs. The red star represents the value for WD 1425 +540, which is a measurement reported in this paper. The ratios for comet Halley, CI chondrites, and bulk Earth are also marked. WD 1425+540 has a very high nitrogen abundance that is comparable to that in comet Halley.

atmosphere provides the first estimate for the bulk nitrogen composition of a rocky/icy planetesimal anywhere, including in our own solar system. Support for the inference that we are measuring a bulk nitrogen concentration comes from the solar-like N/C ratio, suggesting little selective loss of volatiles during the formation and subsequent evolution of the accreted object (Bergin et al. 2015).

The material accreted onto WD 1425+540 is rich in carbon as well, as shown in Table 2. Indeed, carbon is among the most abundant elements comprising the accreted minor planet. Carbon and oxygen are the most abundant heavy elements in planet-forming regions and C/O ratios can influence planetesimal geology. The C/O ratio in WD 1425+540 is 0.15–0.22 by number, indicating that the geology of this planetesimal was dominated by magnesium silicates (Pontoppidan et al. 2014). So far, no extrasolar planetary material with carbon-dominated geology has been detected (Wilson et al. 2016).

Oxygen is the most abundant element in the accreting material. There is an excess of oxygen relative to that which could be bound with the major rock-forming elements, including Mg, Si, Ni, Ca, and Fe. This oxygen excess suggests that the polluting object was not only rich in N and C, presumably as ices, but also in water ice. This is further supported by the large amount of hydrogen in the atmosphere. The amount of excess oxygen is ∼55% by number. If all of the excess oxygen is attributable to H_2O, it would account for $\log n(\mathrm{H})/n(\mathrm{He}) = -6.6$, and the mass fraction of water ice in the object would have been about 30%.

A comet accretion model for white dwarfs was first proposed in Alcock et al. (1986) and more recently discussed in Bonsor et al. (2011) and Stone et al. (2015). However, comet models suffer from various problems (Zuckerman et al. 2003), including derived abundances of heavy elements incompatible with observations. The mass of hydrogen in helium-dominated white dwarfs increases with the white dwarf cooling age, which has been attributed to the accretion of comet-like H_2O rich objects (e.g., Veras et al. 2014). However, the increase of hydrogen abundance could also come from some unexplored evolutionary sequence, such as convective mixing of a thin hydrogen-rich atmosphere below the helium convection zone (Dufour et al. 2007).

The accreting material observed in WD 1425+540 provides direct evidence for the presence of KBO analogs around stars other than the Sun. In addition, WD 1425+540 has a K dwarf companion at 40.0 arcsec (2240 au) away (Wegner 1981). The presence of a distant stellar companion can impact the stability of extended planetary systems and, thus, enhance the chances of perturbing objects—that initially orbit far from a white dwarf—into its tidal radius via the Kozai-Lidov mechanism (Zuckerman 2014; Bonsor & Veras 2015; for a review see Naoz 2016).

When on the main sequence, WD 1425+540 would have had a mass of about $2\,M_\odot$ and a luminosity of $10\,L_\odot$. Thus, the semimajor axes of cold nitrogen-bearing KBOs would have been about 120 au—that is about 3 times further from the star than is the Sun's KBO. Then, mass loss on the AGB would have moved the star's Kuiper Belt out another factor of about 3. Therefore, the object that has been accreted by WD 1425+540 likely was orbiting the white dwarf out beyond 300 au before it began its fateful journey toward oblivion.

4. Perspective

Previous studies show that white dwarfs are mostly accreting from dry, volatile-depleted minor planets. The discovery of a Kuiper-Belt-Object analog, which has polluted the atmosphere of WD 1450+540, provides strong evidence that volatile-rich planetesimals also exist around other stars. In the solar system, significant amounts of volatile compounds and water are present on KBOs, and they could have been important for delivery of these materials to Earth (Morbidelli et al. 2000). With this new data set, we can conclude that extrasolar terrestrial planets could have volatile element and water abundances provided by KBO analogs that are comparable to those on Earth.

This paper is dedicated to the memory of Michael Jura, who was a pioneer in the study of polluted white dwarfs. We thank the anonymous referee for helpful suggestions that improved

the paper. We thank Edwin A. Bergin, Amy Bonsor, Cynthia Genest-Beaulieu, and Pierre Bergeron for interesting discussions. Parts of the data reported here were obtained with the Keck Telescope. The authors wish to recognize and acknowledge the very significant cultural role and reverence that the summit of Mauna Kea has always had within the indigenous Hawaiian community. This research was supported in part by NASA grants to UCLA.

References

Alcock, C., Fristrom, C. C., & Siegelman, R. 1986, ApJ, 302, 462
Allègre, C., Manhès, G., & Lewin, E. 2001, E&PSL, 185, 49
Beichman, C. A., Bryden, G., Stapelfeldt, K. R., et al. 2006, ApJ, 652, 1674
Bergeron, P., Wesemael, F., Dufour, P., et al. 2011, ApJ, 737, 28
Bergin, E. A., Blake, G. A., Ciesla, F., Hirschmann, M. M., & Li, J. 2015, PNAS, 112, 8965
Bonsor, A., Mustill, A. J., & Wyatt, M. C. 2011, MNRAS, 414, 930
Bonsor, A., & Veras, D. 2015, MNRAS, 454, 53
Buie, M. W., Grundy, W. M., Young, E. F., Young, L. A., & Stern, S. A. 2006, AJ, 132, 290
Cruikshank, D. P., Grundy, W. M., DeMeo, F. E., et al. 2015, Icar, 246, 82
Dorn, C., Khan, A., Heng, K., et al. 2015, A&A, 577, A83
Dufour, P., Bergeron, P., Liebert, J., et al. 2007, ApJ, 663, 1291
Dufour, P., Blouin, S., Coutu, S., et al. 2016, ASPC, in press (arXiv: 1610.00986)
Dufour, P., Kilic, M., Fontaine, G., et al. 2010, ApJ, 719, 803
Dufour, P., Kilic, M., Fontaine, G., et al. 2012, ApJ, 749, 6
Farihi, J., Gänsicke, B. T., & Koester, D. 2013, Sci, 342, 218
Gänsicke, B. T., Koester, D., Farihi, J., et al. 2012, MNRAS, 424, 333
Genest-Beaulieu, & Bergeron, P. 2016, ASPC, in press (arXiv:1610.08828)
Greenstein, J. L. 1974, ApJL, 189, L131
Jessberger, E. K., Christoforidis, A., & Kissel, J. 1988, Natur, 332, 691
Jura, M. 2003, ApJL, 584, L91
Jura, M., & Xu, S. 2010, AJ, 140, 1129
Jura, M., & Xu, S. 2012, AJ, 143, 6
Jura, M., Xu, S., Klein, B., Koester, D., & Zuckerman, B. 2012, ApJ, 750, 69
Jura, M., & Young, E. D. 2014, AREPS, 42, 45
Klein, B., Jura, M., Koester, D., & Zuckerman, B. 2011, ApJ, 741, 64
Klein, B., Jura, M., Koester, D., Zuckerman, B., & Melis, C. 2010, ApJ, 709, 950
Koester, D. 2009, A&A, 498, 517
Koester, D., Gänsicke, B. T., & Farihi, J. 2014, A&A, 566, A34
Liebert, J., Gresham, M., Hege, E. K., & Strittmatter, P. A. 1979, AJ, 84, 1612
Lodders, K. 2003, ApJ, 591, 1220
Malamud, U., & Perets, H. B. 2016, ApJ, 832, 160
McSween, H. Y., & Huss, G. R. 2010, Cosmochemistry (Cambridge: Cambridge Univ. Press)
Morbidelli, A., Chambers, J., Lunine, J. I., et al. 2000, M&PS, 35, 1309
Naoz, S. 2016, ARA&A, 54, 441
Pepe, F., Cameron, A. C., Latham, D. W., et al. 2013, Natur, 503, 377
Pontoppidan, K. M., Salyk, C., Bergin, E. A., et al. 2014, in Protostars and Planets VI, ed. H. Beuther et al. (Tucson, AZ: Univ. Arizona Press), 363
Schlegel, D. J., Finkbeiner, D. P., & Davis, M. 1998, ApJ, 500, 525
Stone, N., Metzger, B. D., & Loeb, A. 2015, MNRAS, 448, 188
van Altena, W. F., Lee, J. T., & Hoffleit, D. 1995, yCat, 1174, 0
Veras, D., Shannon, A., & Gänsicke, B. T. 2014, MNRAS, 445, 4175
Vogt, S. S., Allen, S. L., Bigelow, B. C., et al. 1994, Proc. SPIE, 2198, 362
Wasson, J. T., & Kallemeyn, G. W. 1988, RSPTA, 325, 535
Wegner, G. 1981, AJ, 86, 264
Wilson, D. J., Gänsicke, B. T., Farihi, J., & Koester, D. 2016, MNRAS, 459, 3282
Xu, S., Jura, M., Koester, D., Klein, B., & Zuckerman, B. 2014, ApJ, 783, 79
Zuckerman, B. 2014, ApJL, 791, L27
Zuckerman, B., Koester, D., Reid, I. N., & Hünsch, M. 2003, ApJ, 596, 477
Zuckerman, B., Melis, C., Klein, B., Koester, D., & Jura, M. 2010, ApJ, 722, 725